ADVANCES IN FOREST FIRE RESEARCH

2022

Edited by
DOMINGOS XAVIER VIEGAS
LUÍS MÁRIO RIBEIRO

Flame Length of Wildland Fires: Effect of Flame Zone Depth

Mark A. Finney*[1]; Torben P. Grumstrup[1]

[1]*USDA Forest Service Missoula Fire Sciences Laboratory, 5775 Highway 10 West, Missoula MT 59808, USA, {mark.finney, torben.p.grumstup}@usda.gov*

**Corresponding author*

Keywords

Flame length, fireline intensity, flame zone depth

Abstract

Correlations of flame length $\boldsymbol{L}$ with fireline intensity $\boldsymbol{I_B}$, based on theory and data by Thomas (1963), showed that flame zone depth $\boldsymbol{D}$ of a line fire could be neglected if $\boldsymbol{L}$ was much greater than $\boldsymbol{D}$. This has not been verified for wildland fires where $\boldsymbol{D}$ is typically a non-negligible proportion of $\boldsymbol{L}$ (*i.e.*, roughly $\boldsymbol{L/D} < \sim 2$). Here we report on experiments with line-source fires from a gas burner where $\boldsymbol{I_B}$ and $\boldsymbol{D}$ were controlled independently ($0.15 \leq \boldsymbol{L/D} \leq 13.6$). The resulting correlation showed $\boldsymbol{D}$ significantly reduced $\boldsymbol{L}$ for a given $\boldsymbol{I_B}$ over the entire range of observations and was in accord with independent data from spreading fires. Flame length is reduced because the horizontal extent of deep flame zones entrains more air for combustion than assumed by theory involving only the vertical flame profile. Fire behavior modeling that relies on correlations of $\boldsymbol{L}$ with $\boldsymbol{I_B}$ for scaling of heat transfer processes would likely benefit by including the effects of $\boldsymbol{D}$.

1. Introduction

Flame length $\boldsymbol{L}$ (m) of wildland fires is used for modelling heat transfer by radiation (for determining view factor and emissivity) and convection (for determining flame velocity and temperature profiles). It also has practical utility for wildland firefighters as a visual proxy for intensity.

Many empirical studies have shown that $\boldsymbol{L}$ is a power function of Byram's (1959) fireline intensity $\boldsymbol{I_B}$ (kW/m) from linear fire sources such that $\boldsymbol{L \propto c I_B^{\,n}}$. The coefficient $\boldsymbol{c}$ and exponent $\boldsymbol{n}$ in the line fire correlations vary considerably for wildland fires, leading some to suspect the $\boldsymbol{L}$-$\boldsymbol{I_B}$ relationships cannot be compared among fuel types, for example grass vs. shrubland (Alexander 1982; Alexander and Cruz 2012). Importantly, some of the variation in $\boldsymbol{I_B}$ derives from how it is estimated based on Byram's (1959) formula ($\boldsymbol{I_B = H m'' R}$) for spreading fires because of uncertainty in heat yield of the fuel ($\boldsymbol{H}$, kJ/kg), overestimation of fuel mass consumed in flaming per unit area ($\boldsymbol{m''}$, kg/m^2), and sometimes unsteady spread rate $\boldsymbol{R}$ (m/s). Differences have also been attributed to variations in the geometry of the fuel source, fuel material (Steward 1964, Quintiere and Grove 1998) (natural biomass, different hydrocarbon gas, or liquid fuels for example), and the difficulty with obtaining consistent measurements of fluctuating flame length (Zukoski et al. 1986; Newman and Wieczorek 2004).

Data and theory by Thomas (1960, 1963) supported the reasoning that effects of flame zone depth $\boldsymbol{D}$ (m) would become negligible as $\boldsymbol{L}$ greatly exceeded $\boldsymbol{D}$. This paper describes an experiment to test that assumption. We employed a laboratory sand-burner apparatus that allows precise independent control of the gas flow rate and magnitude of flame zone depth $\boldsymbol{D}$.

2. Methods

A propane-fuelled sand burner was constructed at the US Forest Service, Missoula Fire Sciences Laboratory for the purpose of studying flame structure and heat transfer from stationary flame zones (Figure 1). This sand burner is similar to the one described by Finney et al. (2020) but double the size, having rectangular dimensions of the burner box of 1.22 m × 3.66 m. The sand box is 0.15 m deep with 8 perforated tubes running the long axis (3.66 m) along the inside bottom surface under the sand. The burner box is mounted on a tilting platform 3.66 × 7.3 m in size with 4.8 m uphill decking made of flame-resistant Super Fire Temp board 2.54 cm thick.

The downhill decking is 1.2 m (Figure 1) in length. Each tube is controlled separately for gas flowing from a common manifold so that any combination of tubes can be fired with a controlled rate of propane. Gas flow is regulated by an Alicat ® mass flow controller capable of flowing up to 1500 standard liters per minute (SLPM).

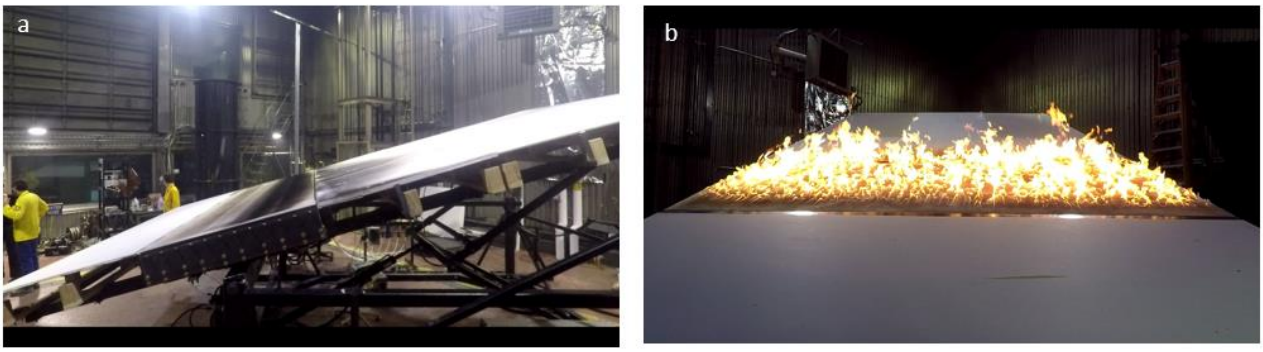

Figure 1- Pictures of propane-fuelled sand burner on a) tilting platform and b) with flames issuing from sandbox.

These experiments were conducted with the platform oriented horizontally so that length of diffusion flames could be measured in the pure vertical dimension. This flame source can be considered buoyancy dominated because the vertical velocity of the propane is so low. Two vertical graduated poles were placed at the foreground edge of the long dimension of the burner in full view of a high-speed camera (Figure 2). The long dimension was chosen because it could more directly incorporate the spatially variable peak and trough structure of line-source flames (Finney et al. 2015) and the non-steady and pulsatile dynamics happening at any given location along a linear flame front (Cetegen et al. 1998). The camera was adjusted to the approximate height of the flames at each setting of propane mass flow rate – 300, 600, 900, 1200, and 1500 SLPM with field of view extending the full 3.66 m width of the burner. For all flow rates, 1-8 burner tubes were opened for 10 seconds of filming.

Video was recorded at 240 frames per second (fps) to minimize smearing from flame movement in each frame. Video was processed to discriminate flaming from non-flaming in each frame using a cut-off brightness value of 90%. Individual binary images were then added to form a probability field for each intensity-flame depth combination and overlayed with a rasterized height gradient determined by the graduated reference poles (Figure 2b). A visual comparison of the video with the probability image suggested that impressions of flame height coincided with the 20% probability contour. For each pixel between the height poles in the image, we obtained the raster height value intersected by the 20% flame presence contour, the mean value of which was an estimate of $\boldsymbol{L}$ (Figure 2c).

Flame length correlations from the gas burner were compared with data from 100 laboratory fires spreading through laser-cut cardboard fuel beds in wind and on a sloping surface (Finney et al. 2013, 2015). Fire spread rate was obtained using thermocouple arrays, flame depth was measured from digital video cameras, and flame length was estimated ocularly. Fireline intensity was calculated from the fuel loading and measured spread rate.

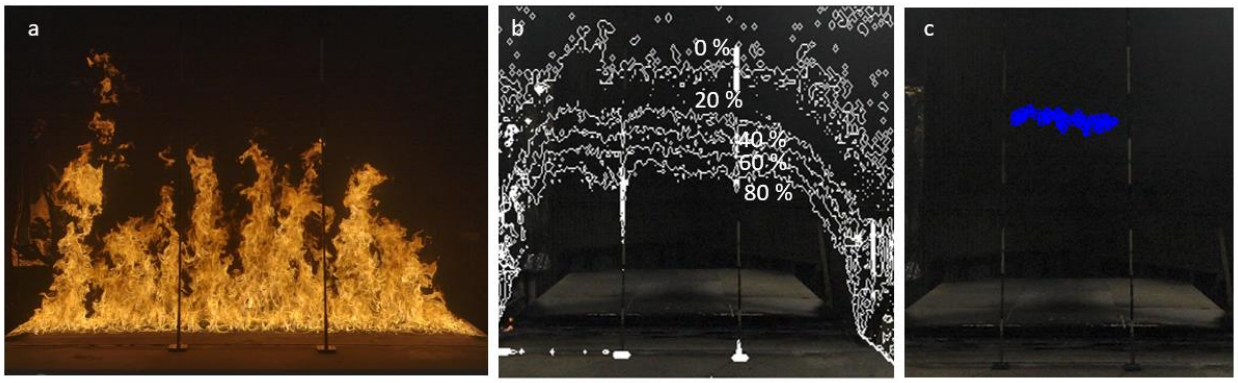

Figure 2 - Image processing of flames is illustrated for a 1200 SLPM gas flow rate with 0.3m flame zone depth D for a) single image of flames from video taken at 240 frames per second showing graduated height poles in the foreground, b) contours of flame presence from 10 seconds of video, and c) points along 20% contour corresponding to an average of $L = 1.55$ m tall (L/D=5.40).

3. Results

The gas burner experiment produced flame length data from a total of 40 combinations of total gas flow rates to the burner (i.e., fireline intensity $\boldsymbol{I_B}$) and number of burner tubes (i.e., flame zone depth $\boldsymbol{D}$) (Table 1). Ratios of $\boldsymbol{L/D}$ ranged from 0.15 to 13.6.

Table 1. Ratios of L/D resulting from experimental combinations of fireline intensity and flame zone depth.

Flame Length/Flame Depth (L/D)								
I_B	**Flame Zone Depth *D* (m)**							
(kW/m)	**0.15**	**0.30**	**0.46**	**0.61**	**0.76**	**0.91**	**1.07**	**1.22**
123	3.20	1.50	0.87	0.60	0.36	0.27	0.20	0.15
246	5.60	2.70	1.73	1.25	0.84	0.67	0.54	0.43
369	9.00	4.30	2.73	1.95	1.40	1.13	0.91	0.78
492	11.20	5.40	3.33	2.40	1.84	1.50	1.23	1.05
615	13.60	6.60	4.27	3.00	2.32	1.80	1.51	1.28

Trends of $\boldsymbol{L}$ as a function of $\boldsymbol{I_B}$ for the gas burner data (thin black curves in Figure 3a) had slopes more like Thomas' (1963) correlation than Byram's (1959). Most importantly, the data showed a strong negative effect of $\boldsymbol{D}$ on the relation of $\boldsymbol{L}$ and $\boldsymbol{I_B}$ for the entire range of variables tested. This is explained using the dimensionless expression of Thomas (1963, eq. 4*ii*):

$$L/D = f(Q'^2/gD^3)^n \quad [1]$$

where $\boldsymbol{Q'}$ is the volumetric flow rate of gas (m^3/s per meter of flame front). Because $\boldsymbol{Q' = I_B/(\rho H)}$, eq. [1] can be rewritten in terms of $\boldsymbol{I_B}$ and absorb the constants into a single coefficient. Using the sand burner data, the empirical coefficient and exponent for the reformulated equation were found by applying nonlinear regression to the experimental data (Figure 3b):

$$L/D = 0.01051\left(I_B^2/D^3\right)^{0.3867} \quad [2]$$

which simplifies to illustrate the significant effect of $\boldsymbol{D}$ on $\boldsymbol{L}$ for the gas burner data:

$$L = 0.01051\left(I_B^{0.774}/D^{0.161}\right) \quad [3]$$

A plot of the burner data shows $\boldsymbol{L}$ was closely predicted by eq. [3] (Figure 3c). Independent data from spreading laboratory fires (Finney et al. 2013, 2015) in Figure 4a showed that when only a function of $\boldsymbol{I_B}$, $\boldsymbol{L}$ was generally overpredicted by Thomas' (1963) correlation and underpredicted by Byram's (1959) at higher intensities. The data trend was well approximated by the correlation from Eq. [3], where $\boldsymbol{L}$ is a function of both $\boldsymbol{I_B}$ and $\boldsymbol{D}$ (Figure 4b).

4. Discussion and Conclusions

The gas burner apparatus allowed precise control over intensity independent of flame source dimensions and revealed the important role of $\boldsymbol{D}$ in determining $\boldsymbol{L}$ in these line-source fires. This result contrasts with Thomas' (1963) data for a similar range ($\boldsymbol{L/D}$ <7) where the exponent for the fitted correlation in eq. [2] (Figure 3b) was found to be 1/3 for $\boldsymbol{L/D}$ > 3 and thus, cancelled the influence of $\boldsymbol{D}$. Steward (1964) also established the theoretical exponent of 1/3 for line fires but experimentally obtained a larger exponent of 0.363 by analysis of a variety of fuel sources for which $\boldsymbol{2 < L/D < 11}$. The flame length data assembled by Quintiere and Grove (1998) largely conform to the 1/3 exponent, but only for $\boldsymbol{L/D > \sim 10}$. Such tall flames with narrow bases are unrealistic for spreading fires in the field and laboratory, suggesting the 1/3 exponent in eq. [2] is not applicable to flames for which $\boldsymbol{L/D < \sim 10}$. Indeed, the following shows that the underlying theory leads one to *expect* an exponent greater than 1/3 for such fires.

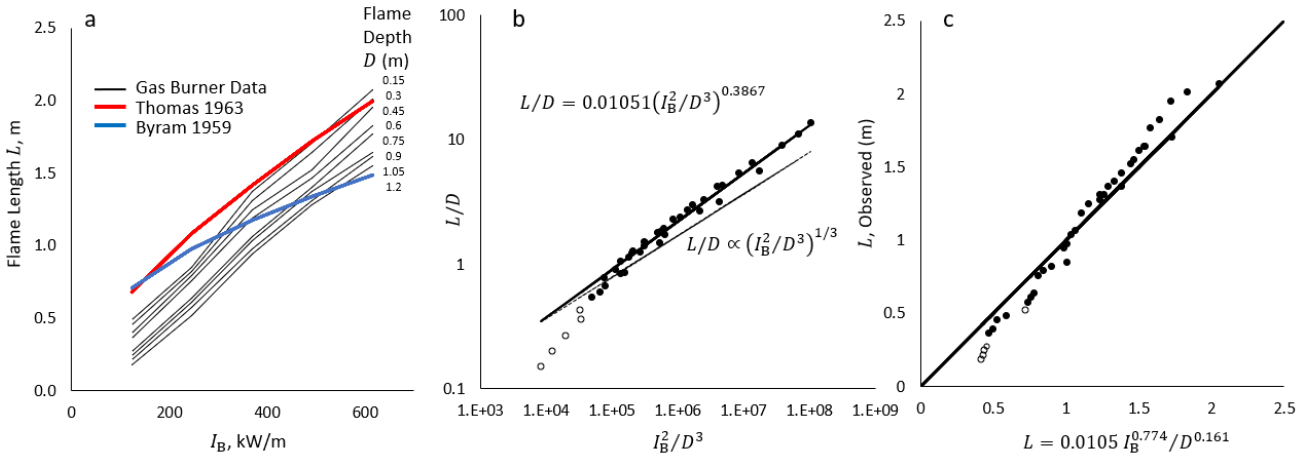

Figure 3. Results of gas burner data a) for flame length L in relation to fireline intensity I_B compared with correlations by Byram (1959) (eq. [1]) and Thomas (1963) (eq. [5]), b) the statistical fit of L/D data compared with Thomas' correlation and c) L observed vs. predicted by eq. [3]. Open circles are observations where L/D<0.52 and flames would likely not form a single plume (Heskestad 1991).

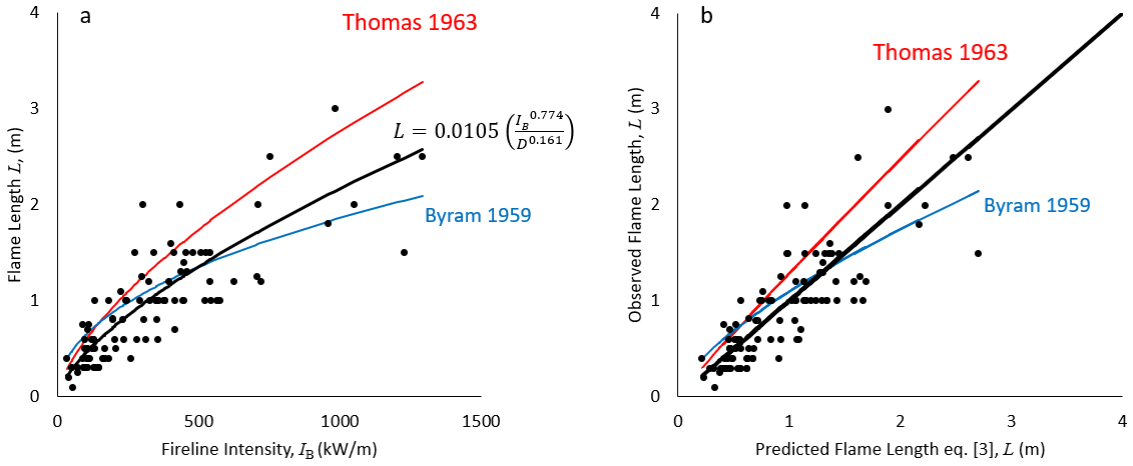

Figure 4. Data from 100 laboratory fires spreading with wind or slope show a) L as a power-function of I_B is generrally overpredicted by the relations of Thomas (1963) (RMSE=0.469) and underpredicted by Byram (1959) at higher intensities (RMSE=0.349), but b) stronger agreement with flame length predicted by eq.[3] (RMSE=0.337).

The roles of $\boldsymbol{I_B}$ and $\boldsymbol{D}$ on $\boldsymbol{L}$ are dependent upon how air is entrained into a turbulent flame. Turbulent entrainment supplies air required for combustion of fuel gases emitted near the ground. Taller flames result from higher fuel flow rates because gases must travel further before adequate mixing allows combustion. Flame length theories have relied upon two principal assumptions. First, air entrainment takes place entirely along the vertical profile of the flame (Thomas 1960, 1963, Steward 1964, Grove and Quintiere 2002, and Nelson et al. 2012). Second, the exterior surface area of the flame profile subjected to air entrainment has been assumed to be linearly proportional to the flame depth and length as would be found if the flames were triangular, rectangular, or trapezoidal. With these assumptions, Thomas (1963) showed that the exponent in equation [1] has the expected value of 1/3, cancelling the effect of $\boldsymbol{D}$ as shown in Figure 3b. This assumption has been assumed to hold where $\boldsymbol{L}$ is much greater than $\boldsymbol{D}$ (Thomas 1963, 1967).

The data in our study clearly contravened the above assumptions because $\boldsymbol{D}$ significantly reduced $\boldsymbol{L}$ in the range $\boldsymbol{0.15 \leq L/D \leq 13.6}$ which is entirely common for spreading wildfires. Published data sets showed median $\boldsymbol{L/D}$ ratios for heading fires of 1.6 (Finney et al. 2013, 2015); 1.4 (Nelson and Adkins 1986, 1988); 0.55 (Catchpole et al. 1998); 1.67 (Sneeuwjagt and Frandsen 1977); and 1.7 (Nelson et al. 2012). However, backing and no-wind fires had greater $\boldsymbol{L/D}$ ratios of 1.81 (Catchpole et al. 1998) and 2.48 (Wilson 1990). All such fires produce inwardly curved flame profiles (Figure 5) that increase entrainment and combustion along much of the horizontal surface in proportion to $\boldsymbol{D}$. Thus, deeper flame zones experience greater combustion of flame gases

traveling along the horizontal fuel bed than allowed by traditional entrainment theory (Thomas 1960, 1963, Steward 1964, Grove and Quintiere 2002, and Nelson et al. 2012) and consequently produce shorter flames for a given intensity. Thomas' (1963) original scaling in equation [1] reflects the increased entrainment with an exponent greater than 1/3, meaning that $\boldsymbol{L}$ depends both on $\boldsymbol{I_B}$ and $\boldsymbol{D}$.

The effect of $\boldsymbol{D}$ on $\boldsymbol{L}$ suggests an important but undescribed negative feedback mechanism that would serve in limiting the spread rate of wildfires. Negative feedbacks are clearly involved in limiting fire spread rate because immediate acceleration of spread and intensity after ignition ultimately gives way to reasonably steady spread. We had earlier reported on the role of $\boldsymbol{D}$ in reducing convective heating through its reduction in the gas temperature profile adjacent to the flaming edge (Finney et al. 2020). A similar effect of $\boldsymbol{D}$ on $\boldsymbol{L}$ would decrease radiation view factor and reduce scaling of convective processes dependent upon flame size, including flame velocity. Both effects of $\boldsymbol{D}$ would work together to dynamically limit fire spread rate as the flame zone depth expands in a spreading fire.

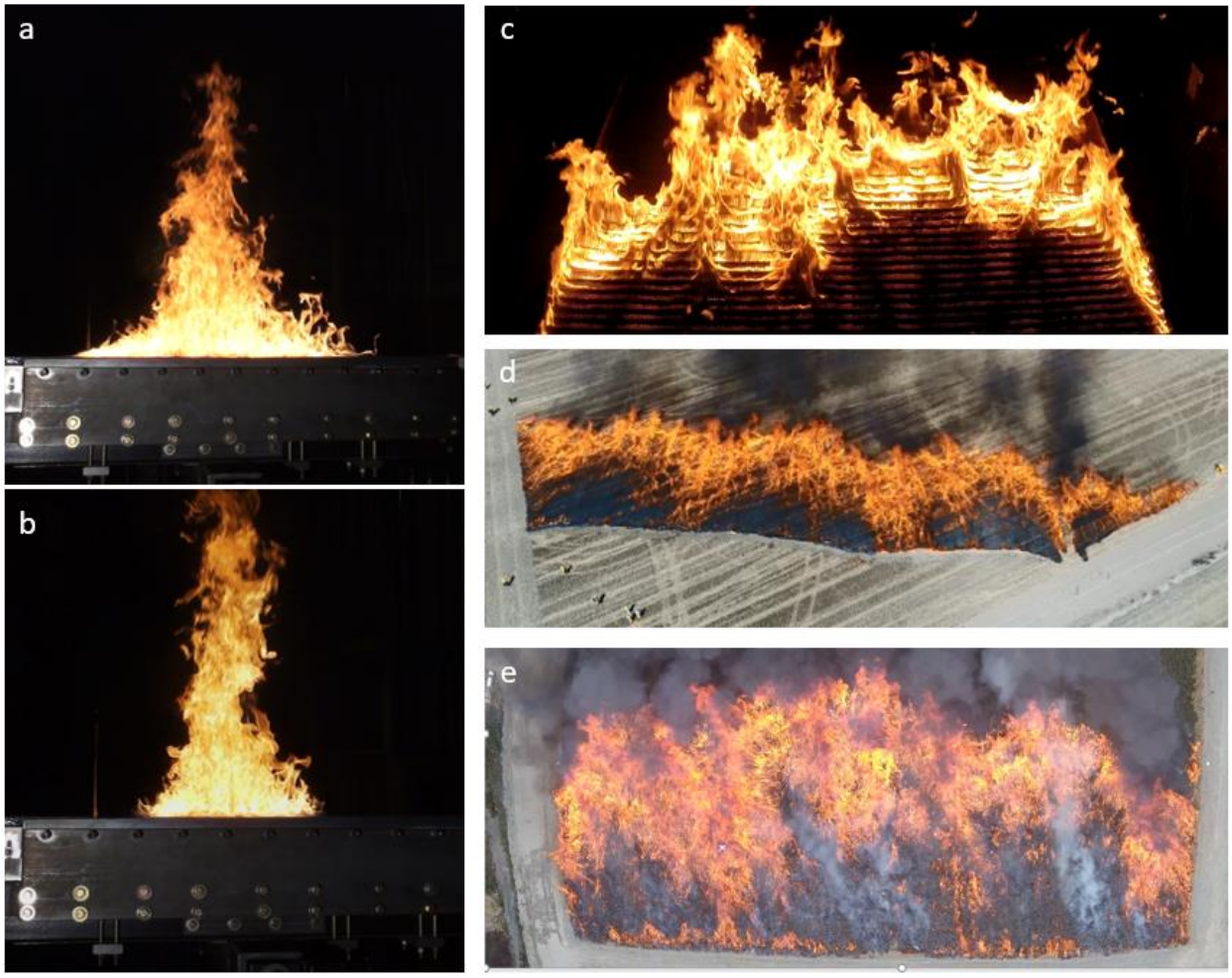

Figure 5. Images of curved flame profiles from gas burner flames a) I_B=205 kW/m; D=0.91m, b) I_B=205 kW/m; D=0.46m. Oblique overhead images of heading fires showing concave flame circulations within flame zones of c) a laboratory fire in laser-cut cardboard (L=0.4m; D=0.4m; $\underline{L/D \cong 1}$; Finney et al. 2015), d) crop stubble fire (L~5m; D~10m; $L/D \cong 0.5$), and e) gorse brush fire in New Zealand (L~15m; D~30m; $L/D \cong 0.5$).

5. Acknowledgements

Research was supported by the USFS, Rocky Mountain Research Station, National Fire Decision Support Centre. The authors thank Jon Bergroos, Ian Grob, and Isaac Grenfell for their assistance with this work.

6. References

Alexander, M.E., 1982. Calculating and interpreting forest fire intensities. *Canadian Journal of Botany*, 60(4), pp.349-357.

Alexander, M.E. and Cruz, M.G., 2012. Interdependencies between flame length and fireline intensity in predicting crown fire initiation and crown scorch height. *International Journal of Wildland Fire*, 21(2), pp.95-113.

Byram, G.M., 1959. Combustion of forest fuels. *Forest fire: control and use*, pp.61-89.

Catchpole, W.R., Catchpole, E.A., Butler, B.W., Rothermel, R.C., Morris, G.A. and Latham, D.J., 1998. Rate of spread of free-burning fires in woody fuels in a wind tunnel. *Combustion Science and Technology*, 131(1-6), pp.1-37.

Cetegen, B.M., Dong, Y. and Soteriou, M.C., 1998. Experiments on stability and oscillatory behavior of planar buoyant plumes. *Physics of Fluids*, *10*(7), pp.1658-1665.

Finney, M.A., Forthofer, J., Grenfell, I.C., Adam, B.A., Akafuah, N.K. and Saito, K., 2013. A study of flame spread in engineered cardboard fuelbeds: Part I: Correlations and observations. In *In: Seventh Intl Symp on Scale Modeling (ISSM-7); Hirosaki, Japan; 6-9 August, 2013. Intl Scale Modeling Committee. 10 p*.

Finney, M.A., Cohen, J.D., Forthofer, J.M., McAllister, S.S., Gollner, M.J., Gorham, D.J., Saito, K., Akafuah, N.K., Adam, B.A. and English, J.D., 2015. Role of buoyant flame dynamics in wildfire spread. *Proceedings of the National Academy of Sciences*, *112*(32), pp.9833-9838.

Finney, M.A., Grumstrup, T.P. and Grenfell, I., 2020. Flame Characteristics Adjacent to a Stationary Line Fire. *Combustion Science and Technology*, pp.1-21.

Finney, M.A., McAllister, S.S., Grumstrup, T.P. and Forthofer, J.M., 2021. Wildland Fire Behaviour: Dynamics, Principles and Processes. CSIRO Publishing, Clayton South, Victoria, Australia, 360 pp.

Grove, B.S. and Quintiere, J.G., 2002. Calculating entrainment and flame height in fire plumes of axisymmetric and infinite line geometries. *Journal of Fire Protection Engineering*, 12(3), pp.117-137.

Heskestad, G., 1991. A reduced-scale mass fire experiment. *Combustion and Flame*, 83(3-4), pp.293-301.

Nelson Jr, R.M. and Adkins, C.W., 1986. Flame characteristics of wind-driven surface fires. *Canadian Journal of Forest Research*, *16*(6), pp.1293-1300.

Nelson Jr, R.M. and Adkins, C.W., 1988. A dimensionless correlation for the spread of wind-driven fires. *Canadian Journal of Forest Research*, *18*(4), pp.391-397.

Nelson, R.M., Butler, B.W. and Weise, D.R., 2012. Entrainment regimes and flame characteristics of wildland fires. *International Journal of Wildland Fire*, *21*(2), pp.127-140.

Newman, J.S. and Wieczorek, C.J., 2004. Chemical flame heights. *Fire safety journal*, 39(5), pp.375-382.

Quintiere, J.G. and Grove, B.S., 1998, January. A unified analysis for fire plumes. In *Symposium (International) on Combustion* 27(2): 2757-2766.

Thomas, P.H., 1960. Buoyant diffusion flames. *Combustion and Flame*, *4*, pp.381-382.

Thomas, P.H., 1963, January. The size of flames from natural fires. In *Symposium (International) on Combustion* (Vol. 9, No. 1, pp. 844-859). Elsevier.

Thomas, P.H., 1967. Some aspects of the growth and spread of fire in the open. *Forestry: An International Journal of Forest Research*, *40*(2), pp.139-164.

Thomas, P.H., Pickard, R.W. and Wraight, H.G., 1963. On the size and orientation of buoyant diffusion flames and the effect of wind. *Fire Safety Science*, *516*, pp.1-1.

Steward, F.R., 1964. Linear flame heights for various fuels. *Combustion and Flame*, 8(3), pp.171-178.

Zukoski, E.E., Cetegen, B.M. and Kubota, T., 1985, January. Visible structure of buoyant diffusion flames. In *Symposium (International) on Combustion* 20(1):361-366.